Turbulent Flow Around a Wing/Fuselage-Type Juncture

L. R. Kubendran*
NASA Langley Research Center, Hampton, Virginia
and
H. M. McMahon† and J. E. Hubbartt†
Georgia Institute of Technology, Atlanta, Georgia

An experimental investigation of a turbulent flowfield in and around a wing/fuselage-type juncture has been made. The results include some measurements taken inside the separated flow region upstream of the wing leading edge. The presence of the wing affects the mean flow distribution upstream of the juncture. The oncoming fuselage boundary layer separates ahead of the wing leading edge, resulting in a vortex that rolls up and trails downstream. In the juncture, the secondary flow system transports turbulence and modifies the mean flow, thus having a large effect on the distribution of turbulent stresses; the separation vortex plays a dominant role in this process. As the downstream distance from the leading edge increases, the vortex diffuses and its core moves away from the juncture. The vortex strength and the streamwise location of the core of the vortex are affected by the slenderness ratio of the wing leading edge. In the juncture flow, there is considerable evidence of similarity between the tubulent shear stresses and the mean flow strain rates. There is also evidence of similarity in the variations of the turbulent stress components.

Nomenclature

u = instantaneous fluctuating velocity
u' = rms fluctuating velocity, i.e., $u' = \sqrt{\overline{u^2}}$
U = local mean or time-averaged velocity
V_∞ = undisturbed freestream velocity
x,y,z = laboratory coordinate system (Fig. 2)
θ = projected mean flow yaw angle (Fig. 2)

Subscripts

x,y,z = component in x, y, z directions

Superscript

$(\bar{})$ = time average or mean

Introduction

IN aircraft design, juncture flows occur at almost all of the orthogonal intersections of surfaces, e.g., wing/fuselage, wing/pylon, tailplane/fuselage, etc. These juncture flows are characterized by the presence of mean flow components in a plane perpendicular to the main flow direction, known as secondary flows. The oncoming turbulent shear layer on the fuselage-type surface skews about an axis parallel to the plane of the mean shear because of the presence of lateral curvature. This results in the generation of streamwise vorticity. Secondary flow due to cross-stream gradients of Reynolds stresses is also present in this turbulent juncture. In addition, as the shear layer approaches the leading edge of the wing, it encounters steep adverse pressure gradients due to the blockage associated with the presence of the wing. These gradients cause the boundary layer to separate ahead of the leading edge, resulting in a vortex that rolls up and trails downstream in the juncture. These combined effects lead to a complex three-dimensional turbulent flow around the juncture.

The secondary flow system occurring in these junctures introduces an incremental drag due to the juncture. More importantly, the secondary vortex system can adversely affect the lift characteristics of some of these surfaces by modifying the regions of attached flow. For example, in the two-dimensional wind tunnel testing of airfoils, the ends of the airfoils are immersed in the sidewall boundary layers. The extent of the two-dimensional region on the airfoil at high angles of attack is significantly affected by the juncture flow.[1] In wing/fuselage-type junctures, the separation vortices trailing in the wake of the wing can alter the lift/drag characteristics of the surfaces downstream.[2] In a similar situation, the wake flow behind the appendages on submarines can degrade the performance of the propeller located downstream.

A clear understanding of this complex juncture flow is necessary in order to evaluate or minimize the abovementioned effects. Researchers involved in computational fluid dynamics consider the analysis of this flow challenging because of the existence of all of the six components of Reynolds stresses and the presence of secondary motion.[3,4] In this context, experimental data are very valuable and can be used in support of numerical modeling of juncture flows.[5,6] In discussing numerical solutions for the turbulent horseshoe vortex flow past strut/end wall configurations, Briley and McDonald[6] indicate that the corner flow analyses should be considered together with the leading-edge horseshoe vortex flow, not in isolation, in order to facilitate modeling of the juncture flow. They also emphasize the need for measurements in the leading-edge region to provide the necessary initial conditions for a numerical solution.

Several of the previous investigations into juncture flows were concerned with flow visualization studies to bring out some of the features of the horseshoe vortex flow.[7,8] In addition, the three-dimensional nature of this flowfield has been studied by several researchers who have made mean flow measurements around the juncture region.[9-11] Detailed measurements also have been carried out in the juncture downstream of the wing leading edge.[12,13] In the present study, measurements of mean velocity components and turbulent stresses have been made in the entire flowfield surrounding the leading edge of a wing/fuselage-type juncture. The effects of the wing leading edge on both the up- and downstream flow regions are examined with the aid of the ex-

Received Dec. 3, 1984; presented as Paper 85-0040 at the AIAA Aerospace Sciences Meeting, Reno, NV, Jan. 14-17, 1985; revision received Jan. 14, 1986.

*NRC-NASA Research Associate, Airfoil Aerodynamics Branch, Transonic Aerodynamics Division. Member AIAA.
†Professor of Aerospace Engineering. Member AIAA.

perimental data. Details of this experimental program are given in Refs. 14-16.

Experiments

Model and Instrumentation

The juncture flow was generated by a constant thickness body ("wing"), having a 1.5:1 elliptical leading edge, which was mounted perpendicular to a large flat plate ("fuselage") and aligned with the freestream (Fig. 1). The thickness of the "wing" was 58 mm. Boundary layers on the wing and the flat plate were tripped using a roughness strip and trip wire, respectively. The incoming "tripped" boundary layer on the plate in an identical setup was studied in detail by Oguz and its quality established in Ref. 13. The experimental setup was located at the exit of an open-return type low-speed wind tunnel.

Two custom-made, single-sensor, hot-wire probes were used for making all of the flow measurements. These probes were oriented with the probe axis perpendicular to the flat plate. The "horizontal" hot-wire probe had the sensor parallel to the plate surface, whereas the "slant" hot-wire probe had its sensor oriented at an angle. In order to minimize the probe interference effects, the hot-wire sensor was supported on needles (0.6 mm diam) protruding through a disk mounted flush with the surface of the flat plate (Fig. 2). The probe calibration procedures are described in Ref. 14.

Operating Conditions

The experiments were carried out at a nominal freestream velocity of 15 m/s corresponding to a Reynolds number of 984,000/m. The flat-plate boundary layer at the wing leading-edge location in the absence of the wing was approximately 23 mm thick, corresponding to a ratio of wing thickness to boundary-layer thickness of 2.5.

Procedure

The streamwise measurement stations used in these experiments are indicated in Fig. 1. The measurements consisted of three mean velocities and six Reynolds stresses. A linearized data analysis scheme[14] was used to obtain these flow quantities.

The need to study the flow very near the leading edge of the wing, where the vortex is formed, required that the measurements be made within a separated flow region. There are two difficulties in making hot-wire measurements in such a region. The first is the problem of encountering a combination of high turbulence level and low mean flow velocity at certain points within this region, which makes the linearized data analysis scheme used in this study inaccurate. Also, there are errors in the mean velocity measurements at low values of the mean velocity because the velocity fluctuations are rectified by the instrument.

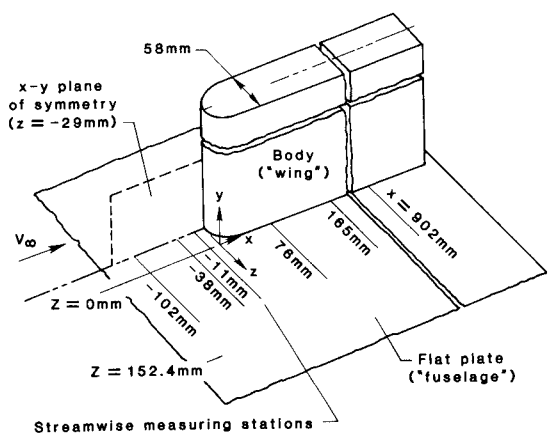

Fig. 1 Experimental model and the locations of streamwise measuring stations.

The second major problem experienced in making hot-wire measurements in a separated, reversed flow region was the ambiguity of the results because of the inability of the hot wire to distinguish between a flow from a given direction and one 180 deg from that direction. This problem was overcome by using a "marching" technique described in Ref. 15. It was reasoned that, as long as the flow direction varies continuously in the marching direction of the probe, it should still be possible to determine the local flow direction even within a separated flow. At the streamwise measuring station $x = -11$ mm, the probe was "marched" in the z direction at constant y by starting at a suitably large value of z where the local yaw angle was approximately known. Using this procedure, it was possible to track successfully the mean of the local flow angle through 180 deg. These flow angles were then used to define the working coordinate system for making the rest of the measurements. The measured flow angles, which close to the plate surface were in very good agreement with surface oil flow visualization, are believed to be reliable. The mean and turbulence quantities measured within the separated region very near the leading edge should be considered qualitative. However, they do provide valuable insights into the details of the separated flow within and near the area of reversed flow and they are good indicators of the trends to be found in such flows.

Results

Upstream Flow Region

Figure 3 shows a vector plot of the mean velocity in the x-y plane of symmetry ($z = -29$ mm) at the three stations upstream of the leading edge. At the furthest upstream station, the velocity profile is less full than for a normal two-dimensional flat-plate boundary layer, indicating that the profile is being influenced by the adverse pressure gradient due to the blockage of the wing. This behavior is more pronounced at $= -38$ mm, but there is no evidence of flow reversal. However, flow reversal has occurred at the measurement sta-

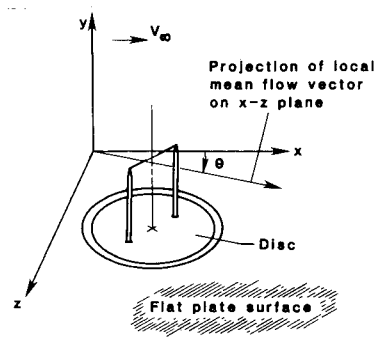

Fig. 2 Typical hot-wire probe arrangement and the coordinate system.

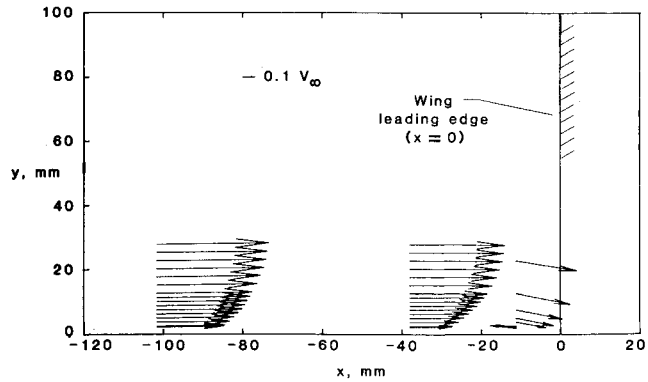

Fig. 3 Vector component plot in x-y plane of symmetry ($z = -29$ mm).

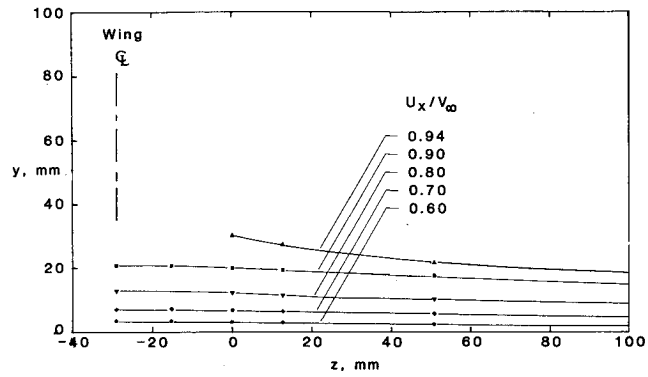

Fig. 4 Contour plot of mean velocity U_x ($x = -102$ mm).

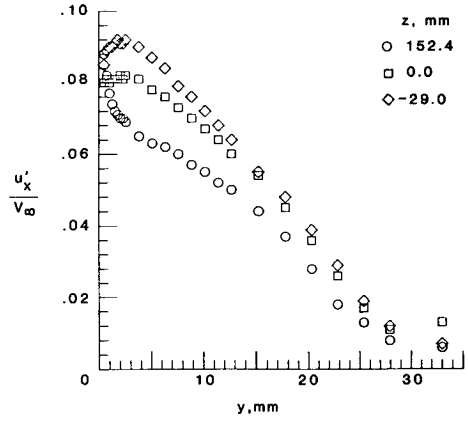

Fig. 5 Turbulent normal stress u_x' upstream of juncture ($x = -38$ mm).

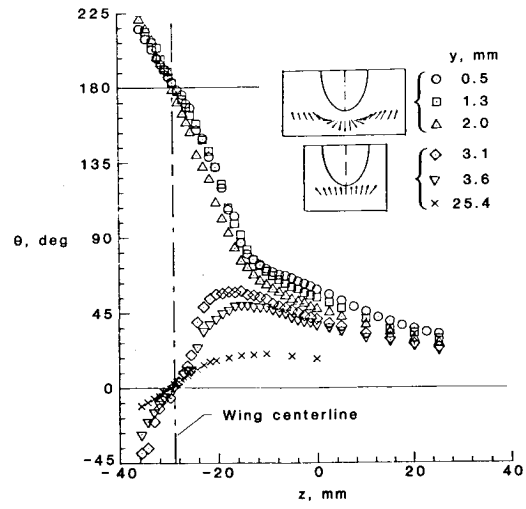

Fig. 6 Variation of local mean flow direction in the vicinity of wing leading edge ($x = -11$ mm).

tion closest to the leading edge of the wing ($x = -11$ mm). In the region above the reversed flow, the velocity vectors are inclined downward. Apparently, this is a manifestation of the impending reattachment and thinning of the shear layer as the boundary layer is swept laterally by the favorable pressure gradients created as a result of the flow around the leading edge of the wing.

A contour plot of the mean velocity U_x at the streamwise station $x = -102$ mm is given in Fig. 4. The deceleration of the oncoming boundary layer at this most upstream station, due to the blockage of the wing, is seen clearly in this figure. In addition to the flow deceleration, boundary-layer skewing was also observed at this measurement station, with a maximum skew angle of $\theta = 6$ deg occurring near the plate surface at about $z = 50$ mm. The magnitude and distribution of the turbulent normal stresses and turbulent shear stresses at $x = -102$ mm are very similar to those in a comparable two-dimensional turbulent boundary layer.

Boundary-layer retardation and skewing are accentuated at the streamwise station $x = -38$ mm. The maximum skewing ($\theta = 30$ deg) occurs outboard of the vertical plane containing the wing surface. The turbulent normal and shear stresses have essentially the same magnitude and distribution as at the measurement station further upstream, with the exception of u_x'. Inboard of the vertical plane containing the wing surface, u_x' has changed because of retardation near the wall, giving rise to a peak in the observed distribution (Fig. 5).

Formation of Separation Vortex

The results of the flow angle measurements carried out at the streamwise station $x = -11$ mm utilizing the "marching" technique referred to earlier are presented in Fig. 6. This figure clearly indicates a reversed flow very near the plate surface within a transverse distance from approximately $z = -15$ mm to the vertical plane of symmetry ($z = -29$ mm). The surveys at the three largest values of y ($y \geq 3$ mm) show that the maximum skew angle is about 50 deg as the flow turns around the wing in the outer part of the viscous region. However, the surveys at the three smallest values of y ($y \leq 2$ mm) indicate a completely different behavior. At approximately $z = -15$ mm, the flow has turned through an angle of 90 deg or at right angles to the original direction. In the plane of symmetry ($z = -29$ mm), the flow angle is 180 deg, meaning that the flow is completely reversed and symmetrical. From these results, it can be estimated that the core of the horseshoe separation vortex lies about 2.5 mm above the surface of the flat plate in the x-y plane of symmetry. Oguz,[13] who used the same experimental setup, concluded from surface static pressure distributions that the effective core is located at $x = -13$ mm in the plane of symmetry.

Profiles of the streamwise mean velocity component U_x at $x = -11$ mm within the separated flow are presented in Fig. 7, where a negative value of U_x denotes a reversed flow. Again, it should be emphasized that these data are qualitative because the measured mean velocities are distorted by the effect of the rectification of the turbulence signals. However, the results are consistent with the other flow quantities measured at this station. A vector plot of the mean velocity component in the y-z plane at this streamwise station is given in Fig. 8. In the plane of symmetry ($z = -29$ mm), the flow is directed downward until very near the plate, where it reverses direction upward. At larger values of z, there is significant downflow in the outer portion of the separated region and a small upflow near the plate surface, indicating the vortex roll-up. At $z = 0$, the transverse component of the mean velocity is comparable to the streamwise component, showing that the flow is turning around the leading edge of the wing.

Profiles of turbulence quantities within the separated region at $x = -11$ mm are given in Ref. 15. For values of $y < 5$ mm, the turbulent shear stresses are very large; the turbulent normal stress u_x'/V_∞ reaches a value of 0.2 near the plate surface at $z = -29$ mm where the mean velocity U_x is also of the same order of magnitude. The turbulent stresses attain values that are comparable to those found in a normal three-dimensional boundary layer, when y exceeds a value of approximately 5 mm.

It can be concluded from the above results that the vortex at its origin is confined to a small region above the plate surface. When describing the laser velocimetry measurements made within a similar flow region, Dickinson[17] arrives at a similar conclusion.

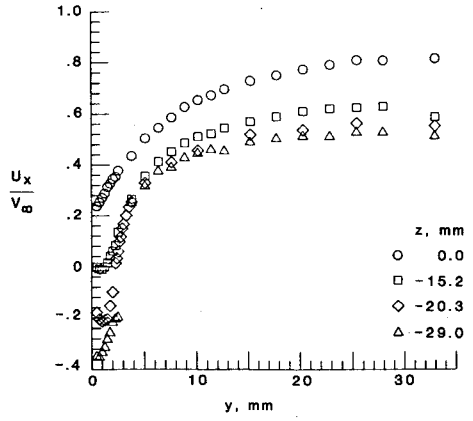

Fig. 7 Mean velocity U_x in the vicinity of wing leading edge ($x = -11$ mm).

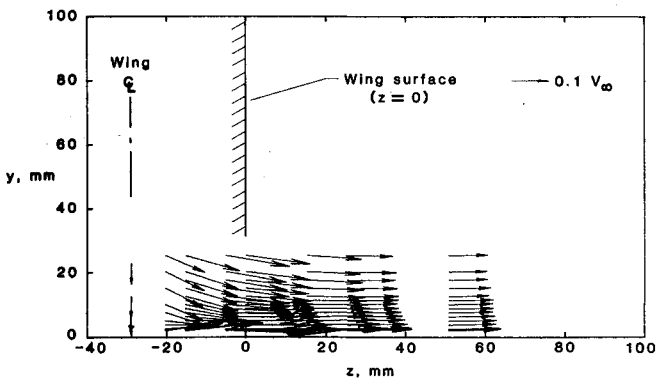

Fig. 8 Vector component plot in y-z plane in the vicinity of wing leading edge ($x = -11$ mm).

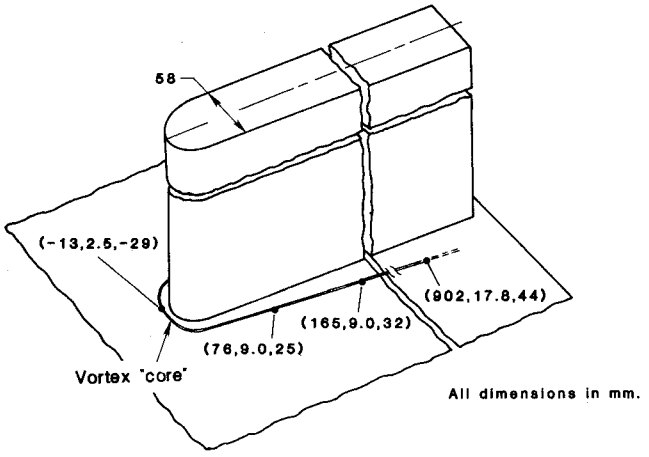

Fig. 9 Estimated trace of the horseshoe vortex core around the juncture (approximately drawn to scale).

Outside of the separated region at this streamwise station ($x = -11$ mm), the boundary layer is thickened near the wing. The skewing component is very large, as seen in Fig. 8. The turbulent normal stresses have changed slightly in response to the retardation and transportation of fluid.

Juncture Flow

Vortex Trace

A sketch of the estimated trace of the separation/vortex core is presented in Fig. 9. At its origin, the vortex core is located very close to the plate surface. Downstream of the leading edge of the wing, the rolled-up vortex has turned and

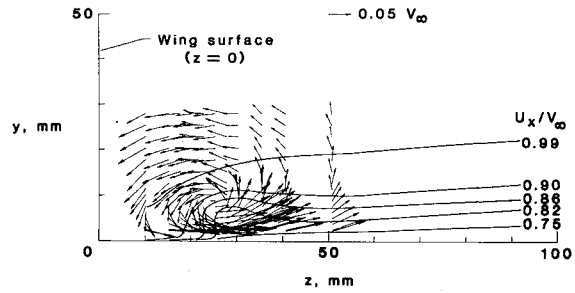

Fig. 10 Contour plot of mean velocity U_x and vector plot of secondary velocities in the juncture ($x = 76$ mm).

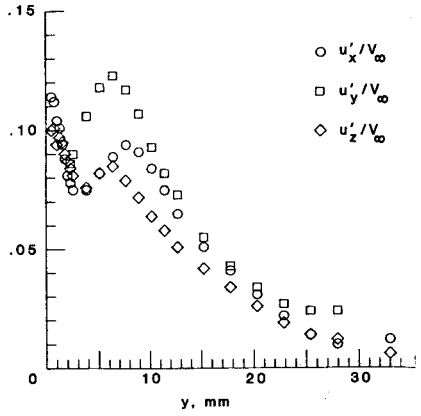

Fig. 11 Turbulent normal stresses in the juncture ($x = 76$ mm, $z = 25.4$ mm).

is trailing downstream; the effective core moves away from the surface of the wing and the surface of the flat plate. The locations of the effective core of the secondary flow vortex have been estimated from secondary flow vector plots at the three streamwise stations in the juncture. Expressed in terms of maximum thickness of the wing, the centers are, respectively, at 0.44, 0.55, and 0.78 wing thicknesses away from the wing surface. In comparison, the weaker vortex (less blunt leading-edge model with a 6:1 slenderness ratio) studied in Ref. 12 was located closer to the wing (0.36 wing thicknesses) at $x = 157$ mm and was only 0.46 wing thicknesses away from the wing at $x = 1223$ mm. In the present case, the vertical y location of the vortex center is located at a value of $y = 9.0$ mm at the first two stations in the juncture and then trails upward to $y = 17.8$ mm. In contrast, the vortex observed in Ref. 12 first moved upward and then downward closer to the horizontal surface as the streamwise distance increased. This may have been due to the presence of favorable pressure gradients in the flow induced by the wall boundary layers, since the experiments of Ref. 12 were conducted in a relatively small wind tunnel.

Mean Velocities and Reynolds Stresses

The measurements in the juncture at $x = 76$ mm are presented in Figs. 10-12. The contour plot of mean velocity U_x in Fig. 10 shows that the counterclockwise (looking downstream) secondary flow transports high-velocity fluid toward the plate near the wing surface and low-velocity fluid upward and away from the plate surface further outboard. The secondary flow also has a large effect on the turbulence quantities. Near the effective core of the secondary flow vortex ($z = 25$ mm), the profiles of turbulent normal stresses are highly distorted (Fig. 11). The profiles of turbulent shear stresses (Fig. 12) also show the pronounced effect of the secondary flow vortex. The components $\overline{u_x u_z}$ and $\overline{u_x u_z}$ are significant. The effect of the vortex even results in a region of negative shear stress $\overline{u_x u_z}$ (i.e., positive values of $\overline{u_x u_z}$) near the plate surface. This region moves away from the wing as the

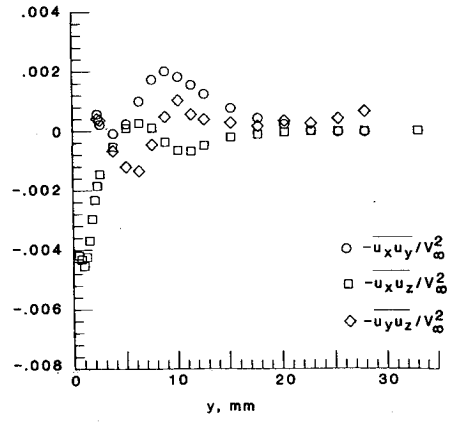

Fig. 12 Turbulent shear stresses in the juncture ($x = 76$ mm, $z = 25.4$ mm).

flow proceeds downstream. The same phenomenon has been reported by Shabaka[12] in a juncture flow featuring a relatively weaker vortex. At the two outer downstream stations $x = 165$ and 902 mm, the effect of the secondary flow vortex on the mean flow and turbulence has progressively diminished. The vortex has also diffused with increasing streamwise distance.

A closer look at Figs. 11 and 12 reveals the presence of similarity in the variations of the turbulent stresses; the similarity in the distributions of turbulent normal stresses u_x' and u_z' (Fig. 11) is particularly striking. This phenomenon was also observed at the streamwise stations $x = 165$ and 902 mm.

Primary Stress Direction

Evaluation of the juncture data also indicated that there is considerable evidence of similarity between the turbulent shear stresses and the mean flow strain rates. This is important in eddy viscosity modeling of shear stresses. A fundamental assumption made in this eddy viscosity concept is that the resultant of the primary stresses $\overline{u_x u_z}$ and $\overline{u_x u_y}$ remain aligned with the mean flow strain rates when the flowfield is distorted.[18] The validity of this assumption is examined in Fig. 13, where the direction of the resultant of shear stresses $\overline{u_x u_z}$ and $\overline{u_x u_y}$ is indicated on the contour plots of streamwise velocity U_x at the streamwise stations $x = 165$ and 902 mm. It can be seen that, for most of the flowfield, the resultant is nearly normal to the velocity contour, even when the effect of the vortex is very strong. Therefore, it may be possible to consider the use of the eddy viscosity model at least in the region of measurements that was covered in this study.

Leading-Edge Shape and Vortex Strength

The results of this study, when compared with those of the works described in Refs. 12 and 19, indicate that the vortex strength is closely related to the slenderness ratio of the leading edge. It may be recalled that a relatively blunt leading edge (slenderness ratio 1.5:1) was used in this study. A semielliptical leading edge of slenderness ratio 6:1 used in Ref. 12 resulted in a weaker vortex, as determined from vector plots of secondary velocities at comparable streamwise stations. The authors of Ref. 19, who used a very slender leading edge (slenderness ratio 12:1), concluded that the secondary flow encountered in the juncture was due mainly to the cross-stream gradients of the Reynolds stresses.

Streamwise Flow Similarities

Comparison of individual mean flow and turbulence quantities measured at the three streamwise stations in the juncture has shown that the profile shapes are essentially similar; the distribution of the quantity with y seems to depend mainly on the position of the profile relative to the vortex core and the vortex intensity. The core location and the vortex strength, in turn, depend on the leading-edge shape as has been noted.

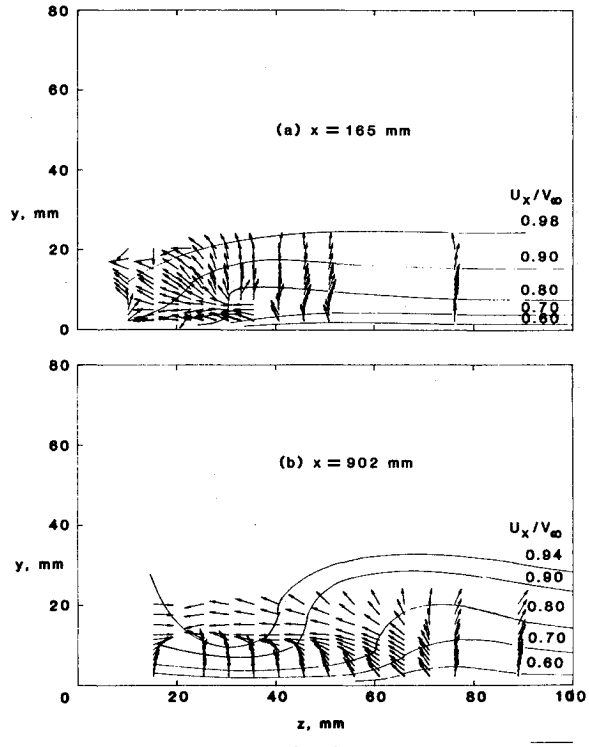

Fig. 13 Direction of resultant of turbulent shear stresses $\overline{u_x u_y}$ and $\overline{u_x u_z}$ with respect to velocity contours of U_x in the juncture.

Conclusions

An important conclusion can be drawn from the results discussed above, namely, that the shape of the leading edge of the wing, especially the slenderness ratio, is the major factor determining the entire flowfield surrounding the juncture. This point is worth keeping in mind when one tries to model this flowfield. The extent to which the mean and turbulence flow quantities in the juncture are affected is dependent on the strength and location of the separation vortex. But, the properties of this vortex, in turn, are related to the leading-edge shape. Therefore, it can be concluded that the strength and location of this horseshoe separation vortex can be controlled by suitably modifying the leading-edge shape of the wing.

There is considerable evidence of similarity between the turbulent shear stresses and the mean flow strain rates and between the variations in the turbulent normal and shear stresses.

Acknowledgment

This work, carried out at the Georgia Institute of Technology, was supported by the NASA Langley Research Center under Grant NAG1-40; Dr. James Scheiman was the technical monitor.

References

[1]Treaster, A. L., Jacob, P. P., and Gurney, G. B., "Correcting for the Sidewall Boundary Layer in Subsonic Two-Dimensional Airfoil/Hydrofoil Testing," AIAA Paper 84-1366, 1984.

[2]Hawthorne, W. R., "The Secondary Flow About Struts and Airfoils," *Journal of the Aeronautical Sciences*, Sept. 1954, pp. 588-608.

[3]Naot, D., Shavit, A., and Wolfshtein, M., "Numerical Calculation of Reynolds Stresses in a Square Duct with Secondary Flow," *Warme-und Stoffubertragung*, Vol. 7, No. 3, 1974, pp. 151-161.

[4]Arnal, D. and Cousteix, J., "Numerical Study of Corner Flows," in: *Three-Dimensional Boundary Layers, Proceedings, International Union of Theoretical and Applied Mechanics Symposium*, Berlin, edited by H. H. Fernholz and E. Krause, Springer-Verlag, Berlin, 1982, pp. 343-352.

[5]Baker, A. J. and Orzechowski, J. A., "An Interaction Algorithm for Three-Dimensional Turbulent Subsonic Aerodynamic Juncture

Region Flow," *AIAA Journal,* Vol. 21, April 1983, pp. 524-533.

[6]Briley, W. R. and McDonald, H., "Computation of Turbulent Horseshoe Vortex Flow Past Swept and Unswept Leading Edges," Scientific Research Associates, Rept. R82-920001-F, (AD-A113534), March 1982.

[7]Rainbird, W. J., Crabbe, R. S., Peake, D. J., and Meyer, R. F., "Some Examples of Separation in Three-Dimensional Flows," *Canadian Aeronautics and Space Journal,* Vol. 12, Dec. 1966, pp. 409-418.

[8]Peake, D. J., Rainbird, W. J., and Atraghji, E. G., "Three-Dimensional Flow Separations on Aircrafts and Missiles," *AIAA Journal,* Vol. 10, May 1972, pp. 567-580.

[9]Hornung, H. G. and Joubert, P. N., "The Mean Velocity Profiles in Three-Dimensional Turbulent Boundary Layers," *Journal of Fluid Mechanics,* Vol. 15, Pt. 3, 1963, pp. 368-385.

[10]East, L. F. and Hoxey, R. P., "Low Speed Three-Dimensional Boundary Layer Data," Pts. 1 and 2, British Advisory Research Council, R&M No. 3653, March 1969.

[11]Prahlad, T. S., "Mean Velocity Profiles in Three-Dimensional Incompressible Turbulent Boundary Layers," *AIAA Journal,* Vol. 11, March 1973, pp. 359-365.

[12]Shabaka, I. M. M. A., "Turbulent Flow in a Simulated Wing/Body Junction," Ph.D. Thesis, Imperial College, London, 1979.

[13]Oguz, E. O., "An Experimental Investigation of the Turbulent Flow in the Junction of a Flat Plate and a Body of Constant Thickness," Ph.D. Thesis, Georgia Institute of Technology, Atlanta, GA, 1980.

[14]McMahon, H., Hubbartt, J., and Kubendran, L., "Mean Velocities and Reynolds Stresses in a Juncture Flow," NASA CR 3605, Aug. 1982.

[15]McMahon, H., Hubbartt, J., and Kubendran, L. R., "Mean Velocities and Reynolds Stresses Upstream of a Simulated Wing-Fuselage Juncture," NASA CR 3695, June 1983.

[16]Kubendran, L. R., "Study of Turbulent Flow in a Wing-Fuselage Type Juncture," Ph D. Thesis, Georgia Institute of Technology, Atlanta, 1983.

[17]Dickinson, S. C., "Flow Visualization and Velocity Measurements in the Separated Region of an Appendage/Flat-plate Junction," Paper presented at Ninth Biennial Symposium on Turbulence, University of Missouri-Rolla, Oct. 1984.

[18]Perkins, H. J., "The Formation of Streamwise Vorticity in Turbulent Flow," *Journal of Fluid Mechanics,* Vol. 44, Pt. 4, 1970.

[19]Kornilov, V. I. and Kharitonov, A. M., "Unsymmetric Corner Flows," *Zhurnal Prikladnoi Mekhaniki i Tekhnicheskoi Fiziki,* No. 2, pp. 44-46, March-April 1983 (translation, Plenum Publishing Corp., New York, 1984).